Materials Research, Vol. 8, No. 1, 45-49, 2005

Fatigue Damage Mechanism and Failure Prevention in Fiberglass Reinforced Plastic

Raimundo Carlos Silverio Freire Jr.[a]*, *Eve Maria Freire de Aquino*[b]*

[a]*CCET, PDCEM, Universidade Federal do Rio Grande do Norte*
Campus Universitário, Lagoa Nova, 59072-970 Natal - RN
[b]*DEM, PPGEM, Univerdade Federal do Rio Garnde do Norte, Centro de Tecnologia*
Campus Universitário, Lagoa Nova, 59072-970 Natal - RN

Receveid: September 3, 2004; Revised: January 17, 2005

Damaging of composite laminates was monitored during fatigue tests, revealing the formation and propagation stages for compressive, tensile, or alternate cyclic loading. Two different laminate stacking sequences, with different number of layers, were tested. The laminates consisted of E-glass fibers reinforced orthoftalic polyester resin (**FGRP**) shaped as mats or (bi-direction) woven fabric textile. Preliminary density, calcination tests and static compressive and tensile mechanical tests were carried out. Then, tensile (**R** = 0.1), compressive (**R** = 10) and alternate axial (**R** = - 1) fatigue tests were performed at different maximum stresses. Tensile cyclic loading resulted in crack formation and propagation confirming the findings reported in other studies. On the other hand, damage from alternate and compressive fatigue depicted peculiar features. Less extended damage and better fatigue resistance were observed for the laminate with symmetrically distributed layers.

Keywords: *fatigue, laminates, FRP composites, damage formation and propagation diagrams*

1. Introduction

Composite laminates in service are submitted to loading, including cyclic loading, which leads to the formation of internal damages, such as matrix fissures, fiber rupture, delamination and microbuckling[1-2]. Several studies[3-7] have addressed the relationships between damage formation and propagation and their negative effect on the mechanical performance of laminates, which reduces the useful life of the material. Reifsnider[3] proposed a diagram which demonstrates the stages of formation and propagation of damage upon fatigue. Transversal cracks are formed in the laminate. Their number increases with the number of cycles up to a saturation limit corresponding to a certain number of cycles. Reifsnider named this saturation limit **CDS** (characteristic damage state). Delamination then takes place and extends leading to full loss of mechanical strength. The composite then fails by fiber rupture.

Gamstedt[8] also developed a model for damage formation and propagation in laminates with transversally oriented fibers with respect to the load direction. In that study, the interface between transversal fibers and matrix was considered as the region with highest susceptibility to damage formation. In addition, the formation of such damages would be different in compression and tension. Finally, alternate loading would significantly decrease the life of the laminate as a result of the combined effect of fiber and matrix debonding under tensile and compressive loads, thus increasing the number of cracks and, consequently, decreasing its strength.

The present study investigates the damage formation and propagation during fatigue tests of two composite laminates with symmetric and asymmetric distribution of E-glass fiber layers in an orthoftalic polyester matrix. Both short fiber mats and bi-direction) woven fabric textile were evaluated. Uniaxial fatigue tests were carried out for **R** = - 1, **R** = 0.1 and **R** = 10. Different maximum applied stresses (**R** is defined as stress ratio, i.e., the ratio between minimum and maximum stress) were also evaluated. Each specimen was tested at constant stress amplitude and high-cycle fatigue, above 10^3 cycles. Uniaxial tensile and compression tests were also carried out in order to determine the ultimate strength of the laminates.

2. Experimental Procedure

The composite materials used herein were manually laminated into 1 m^2 plates. Unsaturated orthoftalic polyester resin was reinforced with both E-glass mats (5 cm, 450 g/m^2) and (bi-direction) woven fabric textile (450 g/m^2). Two plates were then manufactured containing 10 or 12 layers (7 and 10 mm thick, respectively) having the following stacking sequences:

$[M/T/M/T/M]_S$
Stacking sequences of laminate with 10 layers (**C10**)

[*M/T/M/T/M/M/T/M/T/M/T/M*]
Stacking sequences of laminate with 12 layers (**C12**)

where M and T correspond to E-fiberglass mats and (bi-direction) woven fabric textile, respectively, and s refers to the symmetry of the laminate. Only the C10 laminate was symmetric with respect to the distribution of its layers.

The above-mentioned laminates are used by the industry for the manufacturing of reservoirs in general. Originally they are built following the C10 laminate configuration type. However, in order to get better static properties regarding both strength and rigidity around a wall section of the reservoir, two extra layers are laminated and the C12 configuration is obtained. This procedure leads to symmetry problems in that section while the layers are being distributed. According to the results demonstrated in this paper, this practice causes fatigue strength losses for the C12 laminate type.

The fiber contents are virtually identical for both laminates (38.9%). Thus, variations on the mechanical properties or damage formation mechanism can be attributed to the stacking sequence of the composite since the orientation of the fibers (woven fabric) is constant with respect to the direction of the applied load.

*e-mail: freirej@ufrnet.br, eve@dem.ufrn.br

The plates were sectioned using a diamond disk (DIFER D252) to prevent fiber pullout or any other damage. ASTM D 3039 provided the guidelines for the geometry and size of the samples used in the uniaxial tensile tests[9], whereas uniaxial compressive and fatigue samples (R = 10, R = -1 and R = 0.1) were cut according to Mandell[10]. All specimens were rectangular and had the following dimensions: 200 x 25 mm for tensile and fatigue tests, and 100 x 25 mm for compressive tests. Sample gauge was 127 mm for tensile and fatigue tests with R = 0.1; 40 mm for fatigue samples with R = -1, and 35 mm for compression tests with R = 10.

Uniaxial tensile tests were carried out in a universal PAVITEST testing machine and compressive tests in a MTS-810 servo-hydraulic machine. The vertical speed of the plunger was set to 1 mm/min for both series of tests. Five samples were ruptured in each set of static tests. The results, shown in Table 1, revealed that despite the 11% difference in their compressive elastic modulus, the ultimate stresses and elastic moduli of both laminates were nearly identical, yielding similar resistance to static loads.

Fatigue tests were performed using a MTS servo-hydraulic testing machine. The frequency was set to 5 Hz and depicted sinusoidal variation. Stress ratios were R = 0.1, R = - 1 or R = 10. In order to plot S-N curves, maximum tensile stress tests were performed at 60% of the ultimate tensile stress value of the laminate (for R = 0.1 and R = - 1 the ultimate tensile stress was employed whereas ultimate compressive stress was used for R = 10). These results were used to select the maximum stress values used for all other tests. The tests were performed to assure that the number of cycles to failure was between 10^3 and 10^6, thus characterizing high cycle fatigue. Three specimens were tested for each value of maximum stress selected totaling 87 specimens. All tests were carried out at ambient temperature (25 °C) and 50% relative air humidity.

Damage evolution during fatigue tests was assessed by establishing both the number of cycles necessary to stop the propagation of transversal cracks (damage estate) and the number of cycles for delamination. A digital Kodak – Dc215 camera (1100 x 900 pixels resolution) was also used to capture the images necessary to analyze damage formation and propagation across the laminate (free edges).

3. Results

Damage analyses of laminates **C10** and **C12** were carried out for each stress ratio used (**R** = 0.1, **R** = -1 e **R** = 10), since the mechanism of damage formation and propagation depended on this parameter. Damage Formation and Propagation Diagrams (**DFPD**) were then plotted and can be used as a tool to prevent component failure by establishing the conditions of damage initiation for each material.

3.1. Damage analysis of fatigue tests with R = 0.1

DFPDs of laminates **C10** and **C12** tested with **R** = 0.1 are illustrated in Figure 1. Damage occurred in the following stages, which are in good agreement with the results obtained by Reifsnider[3] who carried out damage analyses for unidirectional laminates:

1) Formation of transversal cracks along the entire sample useful area (free edge and width) up to the point of saturation;
2) Propagation of delamination formed by merging transversal cracks;
3) Fiber rupture and ultimate sample fracture described by the **S-N** curve.

Delamination started sooner for laminate **C12** than for laminate **C10**. This was related to the fact that, for the same maximum applied stress, crack saturation was observed under 10^4 cycles for laminate **C12** (Figure 1b) and above that mark for laminate **C10** (Figure 1a) for the same maximum applied stress (σ_{max}). The symmetric distribution of layers allowed better accommodation of internal stresses[11] reducing the number of points of stress concentration and delaying the formation of transversal cracks. As a result, laminate **C10** depicted higher fatigue resistance, which demonstrated the importance of determin-

Table 1. Mechanical properties of laminates **C10** and **C12.**

	Laminate **C10**	Laminate **C12**
Ultimate tensile strength (MPa)	116.7 ± 7.0	115.3 ± 7.7
Ultimate compressive strength (MPa)	171.3 ± 10.0	181 ± 7.1
Tensile elastic modulus (GPa)	4.81 ± 0.61	4.5 ± 0.17
Compressive elastic modulus (GPa)	4.27 ± 0.28	4.79 ± 0.33
Maximum tensile strain (%)	2.45 ± 0.35	2.54 ± 0.24
Maximum compressive strain (%)	4.07 ± 0.41	3.92 ± 0.34

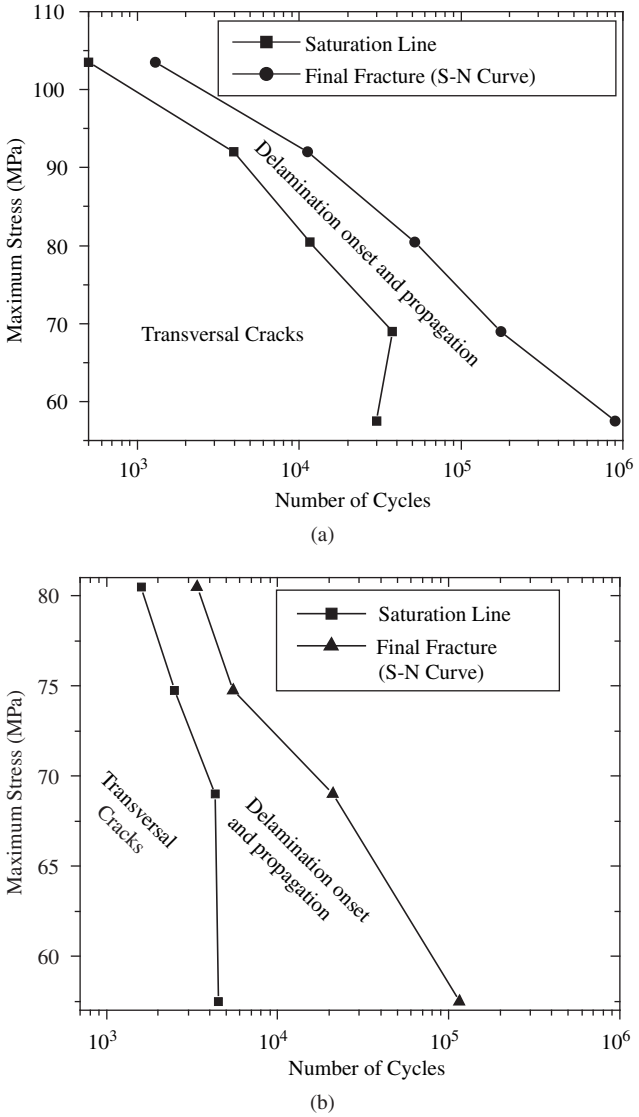

Figure 1. Damage Formation and Propagation Diagrams (DFPD) for laminates: a) C10; b) C12 with R = 0.1.

ing the point of saturation for transversal cracks on the diagnostic of the useful life of laminate composites. In addition, delamination initiated in the inner layers of laminate **C10** and in the outer layers of laminate **C12** probably as a consequence of lower fatigue resistance of the latter. Eventually, rupture of the outer layers of laminate **C12** took place before the ultimate failure of the sample (Figure 2), which was not observed in laminate **C10**.

3.2. Damage analysis for fatigue tests with R = - 1

DFPDs of laminates **C10** and **C12** tested with **R** = -1 are illustrated in Figure 3. The following sequence of events could be established:

1) Formation of transversal cracks;
2) Delamination starting at free edges and subsequent propagation along the width of the sample;
3) Saturation of transversal cracks;
4) Continued formation and propagation of delamination;
5) Fiber rupture and ultimate sample fracture.

Delamination preceded the saturation of transversal cracks and was probably related to the nature of the load applied to the laminates. Since **R** = - 1, laminates underwent alternate tensile – compressive load which prematurely resulted in delamination. This revealed the importance of the type of load applied during fatigue tests on damage formation and propagation of laminates.

Both delamination onset and saturation of transversal cracks took place after fewer cycles for laminate **C12** (500 - 10^4 cycles, Figure 3b) compared to laminate **C10** (10^3 - 10^5 cycles, Figure 3a) for a given applied maximum stress, thus resulting in lower fatigue resistance of laminate **C12**. This was probably related to the symmetry of laminate **C10**, which not only delayed the saturation of transversal cracks but also hindered delamination, mainly in the outer layers of the laminate. This is shown in Figure 4, which portraits a series of images sequentially recorded after various numbers of cycles, **N**, during fatigue test of laminate **C10** submitted to σ_{max} = 69 MPa. The number of cycles to rupture, N_0, was 4400. Delamination occurred in the inner region of laminate **C10** (Figure 4) but randomly for laminate **C12** (Figure 5, **R** = -1, σ_{max} = 46 MPa, N_0 = 17500 cycles).

3.3. Damage analysis for fatigue tests with R = 10

DFPDs of laminates **C10** and **C12** for **R** = 10 are shown in Figure 6. Damage formation and propagation took place in the following order:

1) Delamination started at the free edges.
2) Propagation of delamination along the width of the sample.
3) Fiber rupture followed by ultimate fracture.

No transversal cracks were observed for **R** = 10 in either laminate as a consequence of the essentially cyclic compressive load applied to the laminates. The absence of tensile stresses limited rupture to the final stages of the fracture process. Compared to laminate **C10**, delamination started sooner for laminate **C12**, i.e., between 400 and 10300 cycles for laminate **C12** and between 2100 and 90000 cycles for laminate **C10** for the same maximum applied stress (99.6 - 132.8 MPa). As a result, laminate **C12** depicted shorter useful lifetime. The formation and propagation of delamination along the free edge of laminate **C12** is shown in Figure 7 (σ_{max} = 99.6 MPa, N_0 = 38700 cycles). Delamination occurred in most of its layers, which significantly reduced the useful lifetime of the composite. Conversely, delamination was restricted to the inner layers of laminate **C10** (Figure 8) under similar experimental conditions, resulting in

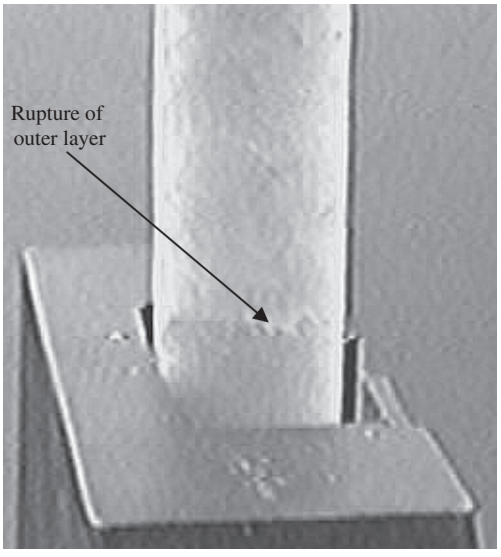

Figure 2. Laminate C12 (σ_{max} = 69 MPa, R = 0.1, N = 18700 cycles, number of cycles to rupture, N_0 = 21200 cycles).

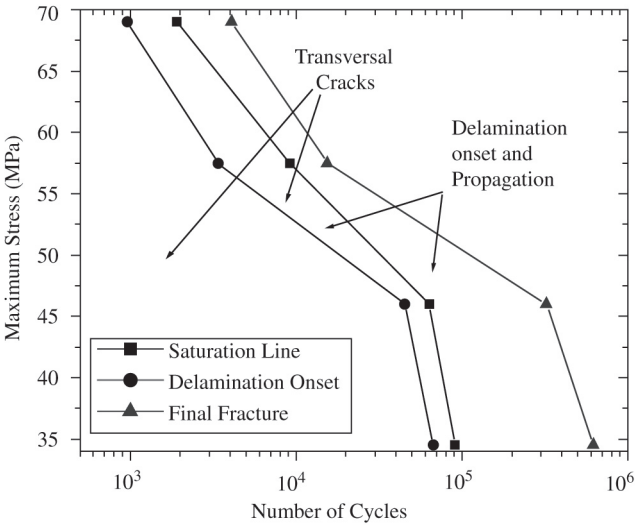

(a)

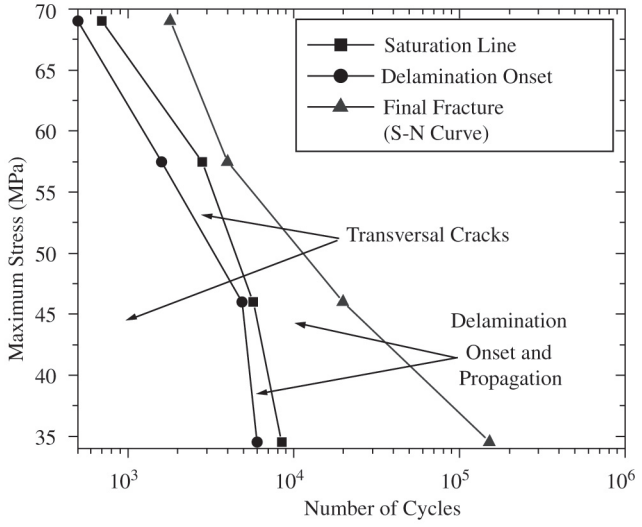

(b)

Figure 3. Damage Formation and Propagation Diagrams (DFPD) for laminate: a) C10; b) C12 with R = -1.

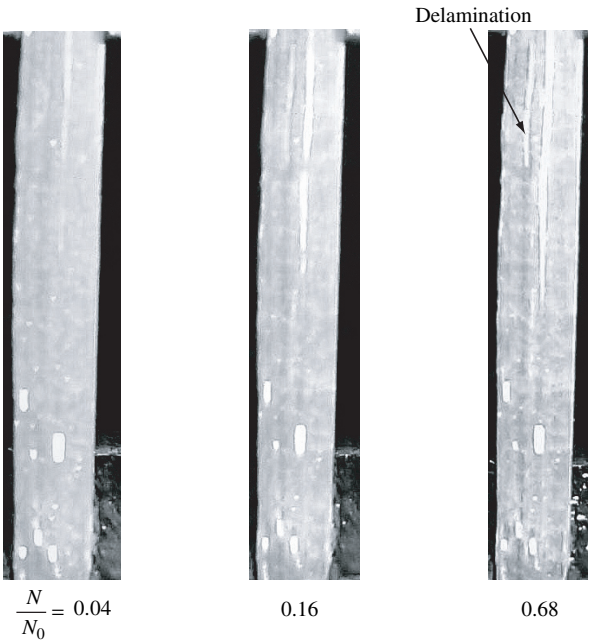

Figure 4. Damage sequence for laminate C10 tested with R = -1 (N_0 = 4400 cycles, σ_{max} = 69 MPa) (free edge region).

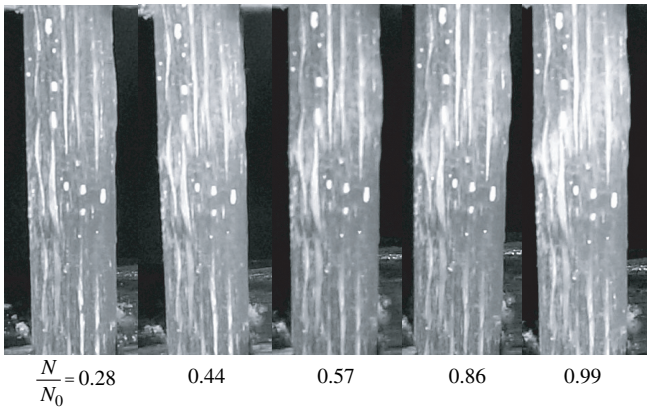

Figure 5. Damage sequence for laminate C12 tested with R = -1 (N_0 = 17500 cycles, σ_{max} = 46 MPa) (free edge region).

longer useful lifetime. The damage sequences of laminates **C10** and **C12** under the same maximum stress (σ_{max} = 132.8 MPa) are illustrated in Figures 8 and 9, respectively. Virtually no sign of damage could be observed in laminate **C10** after 29% of the fatigue test, whereas laminate **C12** revealed extensive delamination of most of its layers after 34% of the test.

4. Conclusions

- For **R** = 0.1 both laminates experienced fatigue damage according to: formation and saturation of transversal cracks, formation and propagation of delamination, fiber rupture and ultimate composite fracture;
- For **R** = -1 the order of the events leading to fracture of both laminates slightly changed to: transversal cracking, formation and propagation of delamination, saturation of transversal cracks, continued formation and propagation of delamination, fiber rupture and ultimate composite fracture;
- For **R** = 10 fracture was restricted to delamination, fiber rupture and ultimate composite fracture;

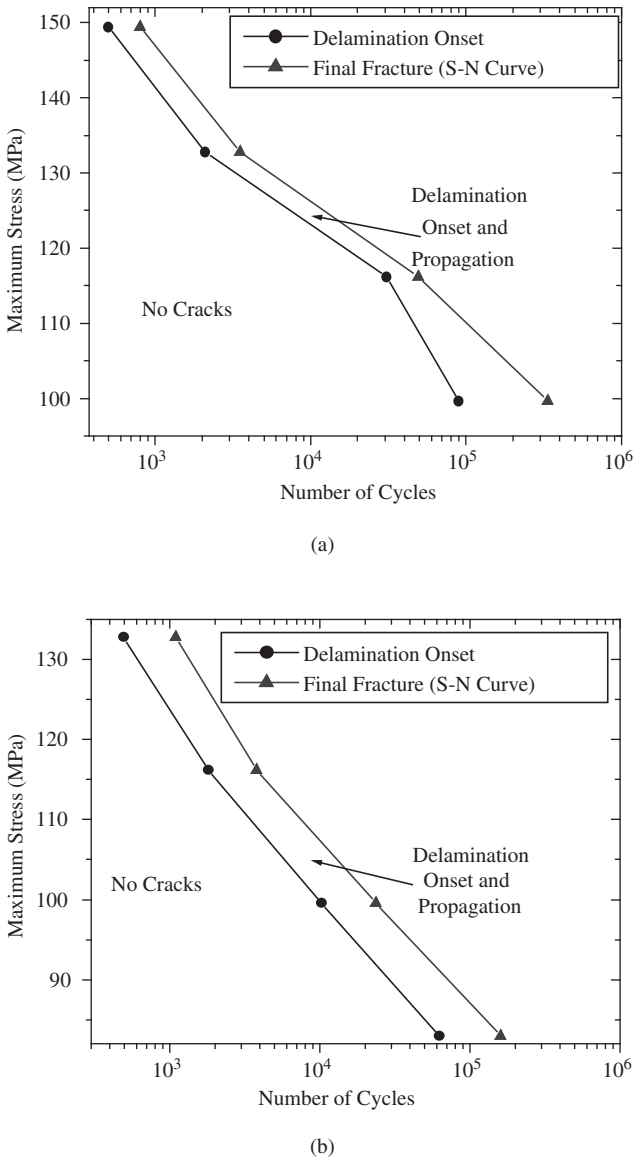

Figure 6. Damage Formation and Propagation Diagrams (DFPD) for laminate (a) C10 and (b) C12 with R = 10.

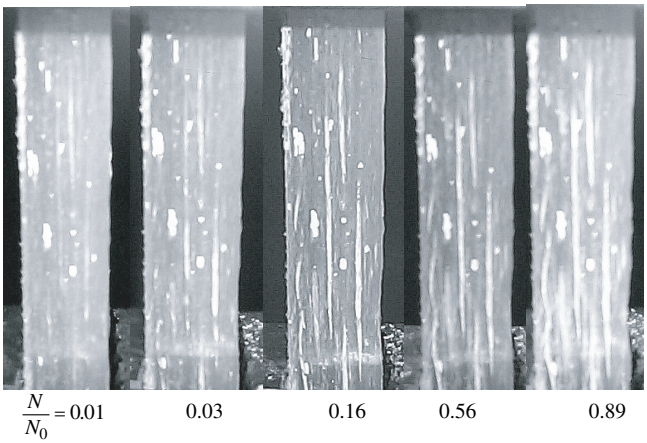

Figure 7. Damage sequence for laminate C12 tested with R = 10 (N_0 = 38700 cycles, σ_{max} = 99.6 MPa).

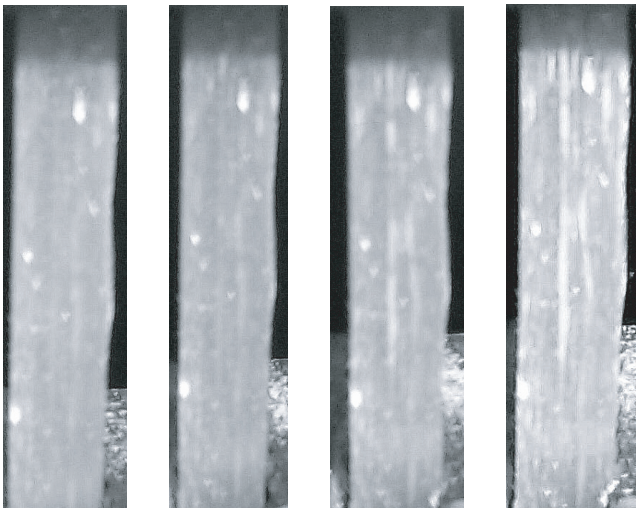

$\frac{N}{N_0} = 0.01$ 0.29 0.57 0.94

Figure 8. Damage sequence for laminate C10 tested with R = 10 (N_0 = 3500 cycles, σ_{max} = 132.8 MPa).

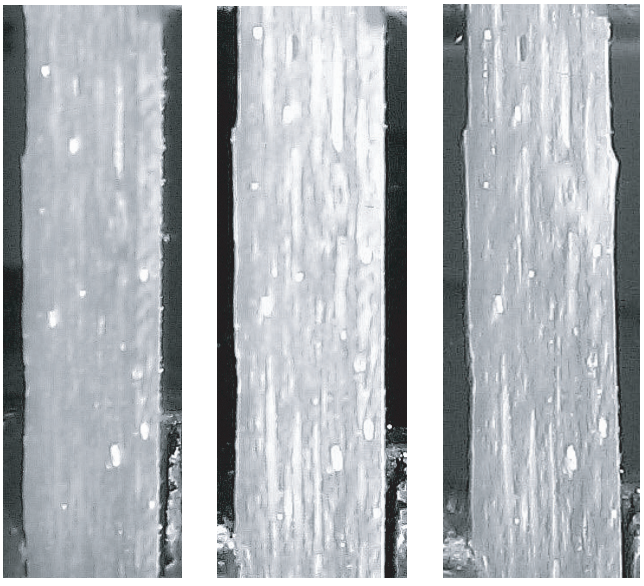

$\frac{N}{N_0} = 0.03$ 0.34 0.48

Figure 9. Damage sequence for laminate C12 tested with R = 10 (N_0 = 1460 cycles, σ_{max} = 132.8 MPa).

- The number of cycles for delamination initiation (for all values of **R** investigated) is directly related to the fatigue resistance, and therefore is helpful to asses to the useful lifetime of the composite;
- Laminate **C12** revealed delamination of inner and especially outer layers whereas delamination of the symmetric laminate **C10** was restricted to its inner layers;
- **DFPDs** are tools to estimate failure prevention or damage formation as a function of the maximum stress and number of cycles.

Acknowledgments

The authors wish to acknowledge CAPES for granting a M.Sc. schorlarship, the Department of Mechanical Engineering of UFPB Campus II for the use of the MTS machine and CEFET – RN for the use of the PAVITEST machine.

References

1. Yang B, Kosey V, Adanur S, Kumar S. Bending, Compression and Shear Behavior of Woven Glass Fiber-Epoxy Composites. *Composites – Part B: Engineering*. 2000; 31:715-721.
2. Felipe RCTS. *Comportamento Mecânico e Fratura de Moldados em PRFV*. [Dissertação de Mestrado]. Natal: Universidade Federal do Rio Grande do Norte; 1997.
3. Reifsnider KL, Henneke EG, Stinchcomb WW, Duke JC. *Mechanics of Composites Materials, Recent Advances*. Ed. Pergamon, 1983.
4. National Institute of Standards and Technology [Director Kammer RG]. *A Fatigue Model for Fiber-Reinforced Polymeric Composites for Offshore Applications*. Blacksburg: Technical Note 1434; 2000.
5. Takeda N, Kobayashi S, Ogihara S, Kobayashi A. Effects of Toughened Interlaminar Layers on Fatigue Damage Progress in Quasi-Isotropic CFRP Laminates. *International Journal of Fatigue*, 1999; 21:235-242.
6. Ogihara S, Takeda N, Kobayashi S, Kobayashi A. Effects of Stacking Sequence on Microscopic Fatigue Damage Development in Quasi-Isotropic CFRP Laminates with Interlaminar-toughened Layers. *Composites Science and Technology*. 1999; 59:1387-1398.
7. Gamstedt EK, Berglund LA, Peijs T. Fatigue Mechanisms in Unidirecional Glass-fibre-reinforced Polypropylene. *Composites Science and Technology*. 1999; 59:759-768.
8. Gamstedt EK, Sjögren BA. Micromechanisms in Tension-Compression Fatigue of Composite Laminates Containing Transverse Plies. *Composites Science and Technology*. 1999; 59:167-178.
9. Standard Test Method for Tensile Properties of Oriented Fiber Composites. ASTM D 3039; 1990.
10. Sandia National Laboratories [Mandell JF, Samborsky DD]. DOE/MSU Composite Material Fatigue Database: Test Methods, Materials and Analysis. Bozeman: Contractor Report SAND97-3002; 1997.
11. Herakovich CT. *Mechanics of Fibrous Composites*. Ed. McGraw-Hill, 1997.